High secondary formation of nitrogen-containing organics (NOCs) and its possible link to oxidized organics and ammonium

Guohua Zhang[1], Xiufeng Lian[1,2], Yuzhen Fu[1,2], Qinhao Lin[1], Lei Li[3], Wei Song[1], Zhanyong Wang[4], Mingjin Tang[1], Duohong Chen[5], Xinhui Bi[1,*], Xinming Wang[1], Guoying Sheng[1]

[1] State Key Laboratory of Organic Geochemistry and Guangdong Provincial Key Laboratory of Environmental Protection and Resources Utilization, Guangzhou Institute of Geochemistry, Chinese Academy of Sciences, Guangzhou 510640, PR China

[2] University of Chinese Academy of Sciences, Beijing 100039, PR China

[3] Institute of Mass Spectrometry and Atmospheric Environment, Guangdong Provincial Engineering Research Center for On-line Source Apportionment System of Air Pollution, Jinan University, Guangzhou 510632, China

[4] School of Intelligent Systems Engineering, Sun Yat-sen University, Shenzhen 518107, PR China

[5] State Environmental Protection Key Laboratory of Regional Air Quality Monitoring, Guangdong Environmental Monitoring Center, Guangzhou 510308, PR China

Correspondence to: Xinhui Bi (bixh@gig.ac.cn)

Highlights

- Nitrogen-containing organics (NOCs) were highly internally mixed with photochemically produced secondary oxidized organics
- NOCs could be well predicted by the variations of these oxidized organics and ammonium
- Higher relative humidity and NOx may facilitate the conversion of these oxidized organics to NOCs

Abstract

Nitrogen-containing organic compounds (NOCs) substantially contribute to light-absorbing organic aerosols, although the atmospheric processes responsible for the secondary formation of these compounds are poorly understood. In this study, seasonal atmospheric processing of NOCs was investigated by single-particle mass spectrometry in urban Guangzhou from 2013-2014. The relative abundance of NOCs is found to be strongly enhanced when internally mixed with the photochemically produced secondary oxidized organics (i.e., formate, acetate, pyruvate, methylglyoxal, glyoxylate, oxalate, malonate, and succinate) and ammonium. Besides, both the hourly detected particle number and relative abundance of NOCs are highly correlated with those of secondary oxidized organics and ammonium. It is therefore hypothesized that secondary formation of NOCs most likely links to the oxidized organics and ammonium. Results from both multiple linear regression analysis and positive matrix factorization analysis further show that the relative abundance of NOCs could be well predicted ($R^2 > 0.7$, $p < 0.01$) by the oxidized organics and ammonium.

Interestingly, the relative abundance of NOCs is inversely correlated with ammonium, whereas their number fractions are positively correlated. This result suggests that although the formation of NOCs does require the involvement of NH_3/NH_4^+, the relative amount of ammonium may have a negative effect. Higher humidity and NOx likely facilitate the conversion of oxidized organics to NOCs. Due to the relatively high oxidized organics and NH_3/NH_4^+, the relative contributions of NOCs in summer and autumn were higher than those in spring and winter. To the best of our knowledge, this is the first direct field observation study

reporting a close association between NOCs and both oxidized organics and ammonium. These findings have substantial implications for the role of ammonium in the atmosphere, particularly in models that predict the evolution and deposition of NOCs.

Keywords: nitrogen-containing organic compounds, individual particles, oxidized organics, ammonium, mixing state, single-particle mass spectrometry

1 Introduction

Organic aerosols that strongly absorb solar radiation are referred to as brown carbon (BrC). BrC has a comparable level of light absorption in the spectral range of near-ultraviolet (UV) light as black carbon (Andreae and Gelencser, 2006; Feng et al., 2013; Yan et al., 2018). Nitrogen-containing organic compounds (NOCs) substantially contribute to the pool of BrC (Mohr et al., 2013; Li et al., 2019), and have a significant effect on atmospheric chemistry, human health and climate forcing (Kanakidou et al., 2005; Shrivastava et al., 2017; De Gouw and Jimenez, 2009). The particulate organic nitrogen accounts for a large fraction of total airborne nitrogen (~30%), although the proportion exhibits a high variability temporally and spatially, and therefore has an influence on both regional and global N deposition (Neff et al., 2002; Shi et al., 2010; Cape et al., 2011). However, the sources, evolution, and optical properties of NOCs remain unclear and contribute significantly to uncertainties in the estimation of their impacts on the environment and climate (Laskin et al., 2015).

NOCs are ubiquitous components of atmospheric aerosols, cloud water and rainwater (Altieri et al., 2009; Desyaterik et al., 2013; Laskin et al., 2015), spanning a wide range of molecular weights, structures and light absorption properties (Lin et al., 2016). Emissions of primary NOCs have been attributed to biomass burning, coal combustion, vehicle emissions, biogenic production and soil dust (Laskin et al., 2009; Desyaterik et al., 2013; Sun et al., 2017; Mace et al., 2003; Rastogi et al., 2011; Wang et al., 2017). Secondary NOCs, such as

organic nitrates and nitroaromatic compounds, are believed to be mainly formed in the gas-phase by interaction between volatile organic compounds and oxidations (e.g., NO_x, ·OH), followed by condensation to aerosols (Ziemann and Atkinson, 2012; Seinfeld and Pandis, 2006). Recently, another type of secondary NOCs, or heterocyclic NOCs, formed by reactions involving mixtures of atmospheric aldehydes (e.g., methylglyoxal/glyoxal) and ammonium/amines are of particular interest (e.g., Hawkins et al., 2016; De Haan et al., 2017; De Haan et al., 2011). A significant portion of heterocyclic NOCs may also be derived from the heterogeneous ageing of secondary organic aerosol (SOA) with NH_3/NH_4^+ (Liu et al., 2015; Laskin et al., 2015). Huang et al. (2017) proposed that even trace levels of ammonia may be sufficient to form heterocyclic NOCs via this pathway. However, these pathways have not been confirmed with ambient data and the relative contribution of heterocyclic NOCs is still uncertain, although they are likely to be minor (at a level of several ng m^{-3}) in abundance (Teich et al., 2016).

The secondary formation of NOCs is especially prevalent in environments experiencing high anthropogenic emissions (Yu et al., 2017; Ho et al., 2015), although further studies are required to establish the formation mechanisms comprehensively. A major obstacle is that organic and inorganic matrix effects have a profound impact on the chemistry of organic compounds in bulk aqueous particles and particles undergoing drying (El-Sayed et al., 2015; Lee et al., 2013). While real-time characterization studies remain a challenge due to the extremely complex chemical nature of NOCs, establishing this data along with the co-variation of NOCs with other chemical components would help to identify the sources and

evolution of NOCs. Using single-particle aerosol time-of-flight mass spectrometry, Wang et al. (2010) observed that the widespread occurrence of NOCs closely correlated with particle acidity in the atmosphere of Shanghai (China). In addition, real-time measurements of the atmosphere in New York (US) by aerosol mass spectrometry indicated a definite link between the age of organic species and the N/C ratio (Sun et al., 2011). Further in-depth studies are required to identify the role of formation conditions (e.g., relative humidity (RH) and pH) for secondary NOCs (Nguyen et al., 2012; Sedehi et al., 2013; Ortiz-Montalvo et al., 2014). In the present study, the mixing state of individual particles was investigated, involving NOCs, oxidized organics, and ammonium, based on on-line seasonal observations using a single particle aerosol mass spectrometry (SPAMS). Our findings show that the formation of NOCs is significantly linked to oxidized organics and NH_4^+, which has important environmental implications for assessing the impact and fate of these compounds.

2 Methods

2.1 Field measurements

Sampling was done at the Guangzhou Institute of Geochemistry, a representative urban site in Guangzhou (China), a megacity in the Pearl River Delta (PRD) region. The size and chemical composition of individual particles were obtained by the SPAMS (Hexin Analytical Instrument Co., Ltd., China) in real-time (Li et al., 2011). The sampling inlet for aerosol characterization was situated 40 meters above the ground level. A brief description of the performance of the SPAMS and other instruments can be found in the Supporting

Information. The sampling periods covered four seasons, including spring (21/02 to 11/04 2014), summer (13/06 to 16/07 2013), autumn (26/09 to 19/10 2013), and winter (15/12 to 25/12 2013). The total measured particle numbers and mean values for meteorological data and gaseous pollutants, are outlined for each season in Table S1 and were described in a previous publication (Zhang et al., 2019).

2.2 SPAMS data analysis

Fragments of NOCs were identified according to the detection of ion peaks at *m/z* -26 $[CN]^-$ or *m/z* -42 $[CNO]^-$, generally due to the presence of C-N bonds (Silva and Prather, 2000; Zawadowicz et al., 2017; Pagels et al., 2013). Laboratory produced C-N bonds compounds from bulk solution-phase reactions between the representative oxidized organics (i.e., methylglyoxal) and ammonium sulfate was used to confirm the generation of ion peaks at *m/z* -26 $[CN]^-$ and/or *m/z* -42 $[CNO]^-$ using SPAMS (Fig. S1). Thus, the NOCs herein may refer to complex nitrated organics such as organic nitrates, nitro-aromatics, nitrogen heterocycles, and polyphenols. Unfortunately, how well $[CN]^-$ / $[CNO]^-$ ions could represent NOCs cannot be quantified, although they were the most commonly reported NOCs peaks by single-particle mass spectrometry (Silva and Prather, 2000; Zawadowicz et al., 2017; Pagels et al., 2013). In the present study, $[CN]^-$ / $[CNO]^-$ ions are among the major peaks detected by the SPAMS (Fig. 1). A rough estimate from the peak area ratio of $[CN]^-$ / $[CNO]^-$ ions and the most likely NOCs fragments (i.e., various amines, and an entire series of nitrogen-containing cluster ions C_nN^-, n = 1, 2, 3, …) (Silva and Prather, 2000) shows that

137 $[CN]^-$ / $[CNO]^-$ ions may represent more than 90% of these NOCs peaks. The number
138 fractions (Nfs) of particles that contained NOCs ranged from 56-59% across all four seasons
139 (Table S1). The number of detected NOC-containing particles as a function of their vacuum
140 aerodynamic diameter (d_{va}) is shown in Fig. S2. Most of the detected NOC-containing
141 particles had a d_{va} in a range of 300-1200 nm.

142 A representative mass spectrum for NOC-containing particles is shown in Fig. 1.
143 Dominant peaks in the mass spectrum were *m/z* 39 $[K]^+$, *m/z* 23 $[Na]^+$, nitrate (*m/z* -62 $[NO_3]^-$
144 or *m/z* -46 $[NO_2]^-$), sulfate (*m/z* -97 $[HSO_4]^-$), organics (*m/z* 27 $[C_2H_3]^+$, *m/z* 63 $[C_5H_3]^+$, *m/z*
145 -42 $[CNO]^-$, *m/z* -26 $[CN]^-$), ammonium (*m/z* 18 $[NH_4]^+$) and carbon ion clusters ($C_n^{+/-}$, n = 1,
146 2, 3,…). NOC-containing particles were internally mixed with various oxidized organics,
147 represented as formate at *m/z* -45 $[HCO_2]^-$, acetate at *m/z* -59 $[CH_3CO_2]^-$, methylglyoxal at
148 *m/z* -71 $[C_3H_3O_2]^-$, glyoxylate at *m/z* -73 $[C_2HO_3]^-$, pyruvate at *m/z* -87 $[C_3H_3O_3]^-$, malonate
149 at *m/z* -103 $[C_3H_3O_4]^-$ and succinate at *m/z* -117 $[C_4H_5O_4]^-$ (Zhang et al., 2017; Zauscher et
150 al., 2013; Lee et al., 2003). These oxidized organics showed their pronounced diurnal trends
151 with afternoon maximum and were highly correlated (r = 0.72 - 0.94, $p < 0.01$) with each
152 other. Therefore, they were primarily attributed to secondary oxidized organics from
153 photochemical oxidation of various volatile organic compounds (VOCs) (Paulot et al., 2011;
154 Zhao et al., 2012; Ho et al., 2011), and the details can be found in our previous publication
155 (Zhang et al., 2019). More information on the seasonal variation range of the Nfs of oxidized
156 organics, ammonium and NOCs is presented in Fig. S3.

Hourly mean Nfs and relative peak areas were applied herein to indicate the variations of aerosol compositions in individual particles. Even though advances have been made in the quantification of specific chemical species for individual particles based on their respective peak area information, it is still quite a challenge for SPAMS to provide quantitative information on aerosol components mainly due to matrix effects, incomplete ionization and so forth (Qin et al., 2006; Jeong et al., 2011; Healy et al., 2013; Zhou et al., 2016). Despite this, the variation of relative peak area should be a good indicator for the investigation of atmospheric processing of various species in individual particles (Wang et al., 2010; Zauscher et al., 2013; Sullivan and Prather, 2007; Zhang et al., 2014).

3 Results and Discussion

3.1 Evidence for the formation of NOCs from oxidized organics and ammonium

Figure 2 shows the seasonal variations in Nfs of the oxidized organics and ammonium, which were internally mixed with NOCs. On average, more than 90% of the oxidized organics and 65% of ammonium (except spring) were found to be internally mixed with NOCs (Fig. S4). Regarding that the Nfs of NOCs relative to all the measured particles was ~60%, it could be concluded that NOCs were enhanced with the presence of oxidized organics and ammonium, with the enhancement associated with oxidized organics being the most pronounced.

A strong correlation between both the Nfs and relative peak areas (RPAs) of NOCs and oxidized organics further demonstrates their close associations, as shown in Fig. 3.

Compared with the oxidized organics, the Nfs of ammonium-containing particles internally mixed with NOCs varied within a broader range (~40-90%). However, there is still an enhancement mixing of NOCs with ammonium. A positive correlation ($R^2 = 0.50$, $p < 0.01$) is observed between the hourly detected number of NOCs and ammonium. It is worth noting that a negative correlation ($R^2 = 0.55$, $p < 0.01$) is obtained between the hourly average RPAs of NOCs and ammonium (Fig. 3).

Based on both the enhancement of NOCs and the high correlations with oxidized organics and ammonium, it is hypothesized that interactions between oxidized organics and ammonium contributed to the observed NOCs. The formation of NOCs from ammonium and carbonyls has been confirmed in several laboratory studies (Sareen et al., 2010; Shapiro et al., 2009; Noziere et al., 2009; Kampf et al., 2016; Galloway et al., 2009). Secondary organic aerosols (SOA) produced from a large group of biogenic and anthropogenic VOCs can be further aged by NH_3/NH_4^+ to generate NOCs (Nguyen et al., 2012; Bones et al., 2010; Updyke et al., 2012; Liu et al., 2015; Huang et al., 2017). In a chamber study, the formation of NOCs is enhanced in an NH_3-rich environment (Chu et al., 2016). While such chemical mechanisms might be complicated, the initial steps generally involve reactions forming imines and amines, which can further react with carbonyl SOA compounds to form more complex products (e.g., oligomers/BrC) (Laskin et al., 2015).

To verify this hypothesis, multiple linear regression analysis is performed to test how well the RPAs of NOCs could be predicted by the oxidized organics and ammonium. As expected, there is a close association ($R^2 = 0.71$, $p < 0.01$) between the predicted RPAs and

199 the observed values of NOCs (Fig. 4), which supports this hypothesis. A noticeable
200 improvement in R^2 implies that a model that uses both oxidized organics and ammonium to
201 predict RPAs of NOCs is substantially better than one that uses only one predictor (either
202 oxidized organics or ammonium in Fig. 3). The result indicates that interactions involving
203 oxidized organics and ammonium could explain over half of the observed variations in
204 NOCs in the atmosphere of Guangzhou. A fraction of the unaccounted NOCs could be due
205 to primary emissions and other formation pathways. This hypothesis could also be supported
206 by a similar pattern of diurnal variation observed for NOCs and oxidized organics (Fig. S5),
207 although there is a slight lag for the NOCs. Such a diurnal pattern is similar to those observed
208 in Beijing and Uintah (Yuan et al., 2016; Zhang et al., 2015). Notably, such a diurnal pattern
209 of secondary NOCs is adequately modelled when the production of NOCs via carbonyls and
210 ammonium is included (Woo et al., 2013). In addition to possible photo-bleaching (Zhao et
211 al., 2015), the lower contribution of NOCs during the daytime may be partly explained by
212 the lower RH, as discussed in section 3.2.

213 Interestingly, the relationship between NOCs and ammonium is distinctly different from
214 the relationship between NOCs and oxidized organics (Fig. 3). This implies that the
215 controlling factors on the formation of NOCs from ammonium are different from oxidized
216 organics. On the one hand, the positive correlation between the detected numbers reflects
217 that the formation of NOCs does require the participant of NH_3/NH_4^+, consistent with the
218 enhancement of NOCs in ammonium-containing particles (Fig. 2) discussed above. On the
219 other hand, the negative correlation between the RPAs signifies that the formation of NOCs

is most probably influenced by the relative amount of ammonium in individual particles. Such influence could also be supported by our data, both from filter samples and individual particle analysis. There is a negative correlation between concentrations of WSON and NH_4^+ for the filter samples (Fig. S6). It can be seen from Fig. S7 that lower RPAs of ammonium correspond to higher Nfs of ammonium that internally mixed with NOCs. Such an inverse correlation could also serve as evidence to explain the influence of the relative amount of ammonium on the formation of NOCs.

The influence of relative ammonium amount on the formation of NOCs is also theoretically possible since the formation of NOCs may be affected by particle acidity (Miyazaki et al., 2014; Nguyen et al., 2012), which is substantially affected by the abundance of ammonium. Consistently, higher relative acidity was observed for the internally mixed ammonium and NOCs particles, compared to ammonium-containing particles without NOCs (Fig. S6) and thus may influence the formation of NOCs (Fig. S7). Particle acidity could also play a significant role in the gas-to-particle partitioning of aldehydes (Herrmann et al., 2015; Liggio et al., 2005; Gen et al., 2018; De Haan et al., 2018; Kroll et al., 2005), precursors for the formation of oxidized organics. However, the higher relative acidity might also be a result of NOCs formation. A model simulation shows that after including the chemistry of SOA ageing with NH_3, an increase in aerosol acidity would be expected due to the reduction in ammonium (Zhu et al., 2018). It is also noted that the particle acidity is roughly estimated by the relative abundance of ammonium, nitrate, and sulfate in individual particles (Denkenberger et al., 2007), and thus may not be representative of actual aerosol

acidity or pH (Guo et al., 2015; Hennigan et al., 2015; Murphy et al., 2017). In addition, ammonia in the gas phase is also efficient at producing NOCs (Nguyen et al., 2012), which may play an intricate role in the distribution of ammonium and NOCs in the particulate phase. The formation of ammonium and NOCs would compete for ammonia, which may also potentially result in the negative correlation between the RPAs of NOCs and ammonium. Unfortunately, such a role remains unclear since the variations of ammonia were not available in the present study.

3.2 Factors contributing to the NOCs resolved by positive matrix factorization (PMF) analysis

Figure 5 presents the PMF factor profiles obtained from the PMF model analysis (detailed information is provided in the SI) (Norris et al., 2009) and their diurnal variations. Around 75% of NOCs could be well explained by two factors, with 33% of the PMF resolved NOCs mainly associated with ammonium and carbonaceous ion peaks (ammonium factor), while 59% were mainly associated with oxidized organics (oxidized organics factor). The explained fraction of NOCs by the ammonium and oxidized organic factors is consistent with the linear regression analysis. Furthermore, PMF analysis provided information on the factor contribution and diurnal variations, which may help explain the seasonal variations and processes of NOCs. The ammonium factor showed a diurnal variation pattern peaking during the early morning, which is consistent with the diurnal variation in RH (Zhang et al., 2019). This factor contributed to ~80% (Fig. S8) of the PMF resolved NOCs during spring

with the highest RH (Table S1), whereas the oxidized organics factor dominated (> 80%) in summer and fall. In winter, these two factors similarly contributed (~40%). Variation of the ammonium factor may reflect a potential role of aqueous pathways in the formation of NOCs, particularly during spring. Differently, the oxidized organics factor showed a pattern of diurnal variation, increasing from morning hours and peaking overnight, which may correspond to the photochemical production of oxidized organics and followed interactions with condensed ammonium. This pathway may explain the slightly late peaking of NOCs compared to oxidized organics, as ammonium condensation is favorable overnight (Hu et al., 2008). While there were similarities in the fractions of oxidized organics in the oxalate factor and the oxidized organics factor, they only contributed to 8% of the PMF resolved NOCs in the oxalate factor, which contained ~80% of the PMF resolved oxalate. As previously discussed, these oxidized organics are also precursors for the formation of oxalate (Zhang et al., 2019). Therefore, the PMF results suggest that there are two competitive pathways for the evolution of these oxidized organics. Some oxidized organics formed from photochemical activities were further oxidized to oxalate, resulting in a diurnal pattern of variation with concentration peaks during the afternoon (Fig. 5), while others interact with NH_3/NH_4^+ to form NOCs, peaking during the nighttime. However, the controlling factors for these pathways could not be determined in the present study. The unexplained NOCs (~25%) might be linked to the primary emissions, such as biomass burning (Desyaterik et al., 2013). It could be partly supported by the presence of potassium and various carbon ion clusters ($C_n^{+/-}$, n = 1, 2, 3, …) in the mass spectrum of NOC-containing particles (Fig. 1).

3.3 Seasonal variations in the observed NOCs

There is an evident seasonal variation of NOCs, with higher relative contributions during summer and autumn (Figs. 3 and 4), mainly due to the variations in oxidized organics and NH_3/NH_4^+. In this region, a more considerable contribution from secondary oxidized organics is typically observed during summer and autumn (Zhou et al., 2014; Yuan et al., 2018). The seasonal maximum NH_3 concentrations have also been reported during the warmer seasons, corresponding to the peak emissions from agricultural activities and high temperatures, while the low NH_3 concentrations observed in colder seasons may be attributed to gas-to-particle conversion (Pan et al., 2018; Zheng et al., 2012). Such seasonal variation in NOCs is also obtained in a model simulation, showing that the conversion of NH_3 into NOCs would result in a significantly higher reduction of gas-phase NH_3 during summer (67%) than winter (31%), due to the higher NH_3 and SOA concentrations present in the summer (Zhu et al., 2018). More primary NOCs may also be present during summer and autumn in the present study, due to the additional biomass burning activities in these seasons (Chen et al., 2018; Zhang et al., 2013).

The seasonal variations of NOCs can be adequately explained by the variations in concentrations of oxidized organics and ammonium (Fig. 4), although the hourly variations during each season are not well explained, as indicated by the lower R^2 values (Table S2). The correlation coefficients (R^2) range from 0.24 to 0.57 for inter-seasonal variations. During spring, NOCs exhibits a limited dependence on oxidized organics (Figs. 3a and 3b),

while during summer, the hourly detected number of NOCs shows a limited dependence on ammonium (Fig. 3d). These seasonal dependences of NOCs are consistent with the PMF results, showing that the ammonium factor explained ~80% of the predicted NOCs during spring, while the oxidized organics factor dominantly contributed to the predicted NOCs during warmer seasons (Fig. S8). A detailed discussion of this issue is provided in the SI.

3.4 Influence of RH and NOx

The influence of RH on RPAs of NOCs and peak ratios of NOCs/oxidized organics are shown in Fig. 6. While NOCs do not show a clear dependence on RH, the ratio of NOCs to the oxidized organics shows an apparent increase towards higher RH. This finding is consistent with the observations reported by Xu et al. (2017), in which the N/C ratio significantly increases as a function of RH in the atmosphere of Beijing. Besides, the diurnal variations of NOCs with peaks values around 20:00 are also similar to those reported by Xu et al. (2017). The peak ratios of NOCs/oxidized organics are more obviously enhanced when RH is higher than 40%. These findings imply that aqueous-phase processing likely plays a substantial role in the formation of NOCs. Significant changes in RH, such as during the evaporation of water droplets, have been reported to facilitate the formation of NOCs via NH_3/NH_4^+ and SOA (Nguyen et al., 2012). In addition, an increase in RH would improve the uptake of NH_3 and the formation of NH_4^+, which also contributes to the enhancement of NOCs. However, the relatively weak correlation ($R^2 = 0.27$, $p < 0.01$) between the peak

ratios and RH, reflect the complex influence of RH on the formation of NOCs (Xu et al., 2017; Woo et al., 2013).

One may expect that NOCs are formed through the interactions between NOx and oxidized organics in the gas phase, followed by condensation (Fry et al., 2014; Ziemann and Atkinson, 2012; Seinfeld and Pandis, 2006). Similar to that observed for RH, while NOCs do not show a clear dependence on NOx (Fig. 6c, R^2 = 0.02–0.13), the ratio of NOCs to the oxidized organics shows a clear increasing trend towards higher NOx (Fig. 6d, R^2 = 0.18, p < 0.01). This indicates that NOx may play a certain role in the conversion of oxidized organics to NOCs, and yet it cannot be quantified in the present study. It is also noted that low correlation coefficients between NOx and NOCs might not indicate a limited contribution of NOx to the formation of NOCs. NOx affects the formation of NOCs in various ways (e.g., peroxy radical chemistry in VOCs oxidation mechanisms and formation of nitrate radicals) (Xu et al., 2015; Zhang et al., 2018), and thus may not linearly contribute to the formation of NOCs.

3.5 Atmospheric implications and limitation

In this study, we showed that in an urban megacity area, secondary NOCs were significantly contributed by the heterogeneous ageing of oxidized organics with NH_3/NH_4^+, providing valuable insight into SOA aging mechanisms. In particular, the effects of NH_3/NH_4^+ on SOA or BrC formation remain relatively poorly understood. In the PRD region, it has been shown that oxygenated organic aerosols (OOA) account for more than 40% of the total

organic mass (He et al., 2011), with high concentrations of available gaseous carbonyls (Li et al., 2014). Therefore, it is expected that over half of all water-soluble NOCs in this region might link to secondary processing (Yu et al., 2017). Furthermore, secondary sources have been found to contribute significantly to NOCs related BrC in Nanjing, China (Chen et al., 2018). The results presented herein also suggest that the production of NOCs might be adequately estimated by their correlation with secondary oxidized organics and ammonium. The effectiveness of correlation-based estimations needs to be examined in other regions before being generally applied in other environments. However, this approach may provide valuable insights into investigations of NOCs using atmospheric observations. In contrast, it has previously been reported that a positive correlation exists between WSON and ammonium (Li et al., 2012), indicating similar anthropogenic sources. This divergence could be mainly attributed to varying contributions of primary sources and secondary processes to the observed NOCs. Possible future reductions in anthropogenic emissions of ammonia may reduce particle NOCs. Understanding the complex interplay between inorganic and organic nitrogen is an essential part of assessing global nitrogen cycling.

Moise et al. (2015) proposed that with high concentrations of reduced nitrogen compounds, high photochemical activity, and frequent changes in humidity, BrC formed via NH_3/NH_4^+ and SOA may become a dominant contributor to aerosol absorption, specifically in agricultural and forested areas. However, this study suggests that even in typical urban areas, BrC formation via NH_3/NH_4^+ and SOA should not be neglected. In particular, SOA was found to account for 44 – 71% of the organic mass in megacities across China (Huang

et al., 2014), with NH_3 concentrations in urban areas comparable with those from agricultural sites and 2- or 3-fold those of forested areas in China (Pan et al., 2018). Additionally, the acidic nature of particles in these regions would also be favorable for the formation of NOCs (Guo et al., 2017; Jia et al., 2018). Considering the formation of NOCs from the uptake of NH_3 onto SOA particles, Zhu et al. (2018) suggested that this mechanism could have a significant impact on the atmospheric concentrations of NH_3/NH_4^+ and NO_3^-.

5 Conclusions

This study investigated the processes contributing to the seasonal formation of NOCs, involving ammonium and oxidized organics in urban Guangzhou, using single-particle mass spectrometry. This is the first study to provide direct field observation results to confirm that the variation of NOCs correlate well and are strongly enhanced internal mixing with secondary oxidized organics. These findings highlight the possible formation pathway of NOCs through the ageing of secondary oxidized organics by NH_3/NH_4^+ in ambient urban environments. A clear pattern of seasonal variation in NOCs was observed, with higher relative contributions in summer and autumn as compared to spring and winter. This seasonal variation was well predicted by multiple linear regression model analysis, using the relative abundance of oxidized organics and ammonium as model inputs. More than 50% of NOCs could be explained by the interaction between oxidized organics and ammonium. The production of NOCs through such processes was facilitated by increased humidity and NOx. These results extend our understanding of the mixing state and atmospheric processing of

particulate NOCs, as well as having substantial implications for the accuracy of models predicting the formation, fate, and impacts of NOCs in the atmosphere.

Author contribution

GHZ and XHB designed the research (with input from WS, LL, ZYW, DHC, MJT, XMW and GYS), analyzed the data, and wrote the manuscript. XFL, YZF, and QHL conducted air sampling work and laboratory experiments under the guidance of GHZ, XHB and XMW. All authors contributed to the refinement of the submitted manuscript.

Acknowledgement

This work was supported by the National Nature Science Foundation of China (No. 41775124 and 41877307), the National Key Research and Development Program of China (2017YFC0210104 and 2016YFC0202204), the Science and Technology Project of Guangzhou, China (No. 201803030032), and the Guangdong Foundation for Program of Science and Technology Research (No. 2017B030314057).

References

Altieri, K. E., Turpin, B. J., and Seitzinger, S. P.: Composition of Dissolved Organic Nitrogen in Continental Precipitation Investigated by Ultra-High Resolution FT-ICR Mass Spectrometry, Environ. Sci. Technol., 43, 6950-6955, doi:10.1021/es9007849, 2009.

Andreae, M. O., and Gelencser, A.: Black carbon or brown carbon? The nature of light-absorbing carbonaceous aerosols, Atmos. Chem. Phys., 6, 3131-3148, 2006.

Bones, D. L., Henricksen, D. K., Mang, S. A., Gonsior, M., Bateman, A. P., Nguyen, T. B., Cooper, W. J., and Nizkorodov, S. A.: Appearance of strong absorbers and fluorophores in limonene-O_3 secondary organic aerosol due to NH_4^+-mediated chemical aging over long time scales, J. Geophys. Res.-Atmos., 115, D05203, doi:10.1029/2009jd012864, 2010.

Cape, J. N., Cornell, S. E., Jickells, T. D., and Nemitz, E.: Organic nitrogen in the atmosphere — Where does it come from? A review of sources and methods, Atmos. Res., 102, 30-48, doi:10.1016/j.atmosres.2011.07.009, 2011.

Chen, Y. F., Ge, X. L., Chen, H., Xie, X. C., Chen, Y. T., Wang, J. F., Ye, Z. L., Bao, M. Y., Zhang, Y. L., and Chen, M. D.: Seasonal light absorption properties of water-soluble brown carbon in atmospheric fine particles in Nanjing, China, Atmos. Environ., 187, 230-240, doi:10.1016/j.atmosenv.2018.06.002, 2018.

Chu, B. W., Zhang, X., Liu, Y. C., He, H., Sun, Y., Jiang, J. K., Li, J. H., and Hao, J. M.: Synergetic formation of secondary inorganic and organic aerosol: effect of SO_2 and NH_3 on particle formation and growth, Atmos. Chem. Phys., 16, 14219-14230, doi:10.5194/acp-16-14219-2016, 2016.

De Gouw, J., and Jimenez, J. L.: Organic Aerosols in the Earth's Atmosphere, Environ. Sci. Technol., 43, 7614-7618, doi:10.1021/Es9006004, 2009.

De Haan, D. O., Hawkins, L. N., Kononenko, J. A., Turley, J. J., Corrigan, A. L., Tolbert, M. A., and Jimenez, J. L.: Formation of Nitrogen-Containing Oligomers by Methylglyoxal and Amines in Simulated Evaporating Cloud Droplets, Environ. Sci. Technol., 45, 984-991, doi:10.1021/es102933x, 2011.

De Haan, D. O., Hawkins, L. N., Welsh, H. G., Pednekar, R., Casar, J. R., Pennington, E. A., de Loera, A., Jimenez, N. G., Symons, M. A., Zauscher, M., Pajunoja, A., Caponi, L., Cazaunau, M., Formenti, P., Gratien, A., Pangui, E., and Doussin, J.-F.: Brown Carbon Production in Ammonium- or Amine-Containing Aerosol Particles by Reactive Uptake of Methylglyoxal and Photolytic Cloud Cycling, Environ. Sci. Technol., 51, 7458-7466, doi:10.1021/acs.est.7b00159, 2017.

De Haan, D. O., Jimenez, N. G., de Loera, A., Cazaunau, M., Gratien, A., Pangui, E., and Doussin, J.-F.: Methylglyoxal Uptake Coefficients on Aqueous Aerosol Surfaces, J. Phys. Chem. A, 122, 4854-4860, doi:10.1021/acs.jpca.8b00533, 2018.

Denkenberger, K. A., Moffet, R. C., Holecek, J. C., Rebotier, T. P., and Prather, K. A.: Real-time, single-particle measurements of oligomers in aged ambient aerosol particles, Environ. Sci. Technol., 41, 5439-5446, doi:10.1021/es070329l, 2007.

Desyaterik, Y., Sun, Y., Shen, X., Lee, T., Wang, X., Wang, T., and Collett, J. L., Jr.: Speciation of "brown" carbon in cloud water impacted by agricultural biomass burning in eastern China, J. Geophys. Res.-Atmos., 118, 7389-7399, doi:10.1002/jgrd.50561, 2013.

El-Sayed, M. M. H., Wang, Y. Q., and Hennigan, C. J.: Direct atmospheric evidence for the irreversible formation of aqueous secondary organic aerosol, Geophys. Res. Lett., 42, 5577-5586, doi:10.1002/2015gl064556, 2015.

Feng, Y., Ramanathan, V., and Kotamarthi, V. R.: Brown carbon: a significant atmospheric absorber of solar radiation?, Atmos. Chem. Phys., 13, 8607-8621, doi:10.5194/acp-13-8607-2013, 2013.

Fry, J. L., Draper, D. C., Barsanti, K. C., Smith, J. N., Ortega, J., Winkle, P. M., Lawler, M. J., Brown, S. S., Edwards, P. M., Cohen, R. C., and Lee, L.: Secondary Organic Aerosol Formation and Organic Nitrate Yield from NO3 Oxidation of Biogenic Hydrocarbons, Environ. Sci. Technol., 48, 11944-11953, doi:10.1021/es502204x, 2014.

Galloway, M. M., Chhabra, P. S., Chan, A. W. H., Surratt, J. D., Flagan, R. C., Seinfeld, J. H., and Keutsch, F. N.: Glyoxal uptake on ammonium sulphate seed aerosol: reaction

products and reversibility of uptake under dark and irradiated conditions, Atmos. Chem. Phys., 9, 3331-3345, doi:10.5194/acp-9-3331-2009, 2009.

Gen, M., Huang, D. D., and Chan, C. K.: Reactive Uptake of Glyoxal by Ammonium-Containing Salt Particles as a Function of Relative Humidity, Environ. Sci. Technol., 52, 6903-6911, doi:10.1021/acs.est.8b00606, 2018.

Guo, H., Xu, L., Bougiatioti, A., Cerully, K. M., Capps, S. L., Hite, J. R., Carlton, A. G., Lee, S. H., Bergin, M. H., Ng, N. L., Nenes, A., and Weber, R. J.: Fine-particle water and pH in the southeastern United States, Atmos. Chem. Phys., 15, 5211-5228, doi:10.5194/acp-15-5211-2015, 2015.

Guo, H., Weber, R. J., and Nenes, A.: High levels of ammonia do not raise fine particle pH sufficiently to yield nitrogen oxide-dominated sulfate production, Sci. Rep., 7, 12109, doi:10.1038/s41598-017-11704-0, 2017.

Hawkins, L. N., Lemire, A. N., Galloway, M. M., Corrigan, A. L., Turley, J. J., Espelien, B. M., and De Haan, D. O.: Maillard Chemistry in Clouds and Aqueous Aerosol As a Source of Atmospheric Humic-Like Substances, Environ. Sci. Technol., 50, 7443-7452, doi:10.1021/acs.est.6b00909, 2016.

He, L. Y., Huang, X. F., Xue, L., Hu, M., Lin, Y., Zheng, J., Zhang, R. Y., and Zhang, Y. H.: Submicron aerosol analysis and organic source apportionment in an urban atmosphere in Pearl River Delta of China using high-resolution aerosol mass spectrometry, J. Geophys. Res.-Atmos., 116, 1-15, doi:10.1029/2010jd014566, 2011.

Healy, R. M., Sciare, J., Poulain, L., Crippa, M., Wiedensohler, A., Prevot, A. S. H., Baltensperger, U., Sarda-Esteve, R., McGuire, M. L., Jeong, C. H., McGillicuddy, E., O'Connor, I. P., Sodeau, J. R., Evans, G. J., and Wenger, J. C.: Quantitative determination of carbonaceous particle mixing state in Paris using single-particle mass spectrometer and aerosol mass spectrometer measurements, Atmos. Chem. Phys., 13, 9479-9496, doi:10.5194/acp-13-9479-2013, 2013.

Hennigan, C. J., Izumi, J., Sullivan, A. P., Weber, R. J., and Nenes, A.: A critical evaluation of proxy methods used to estimate the acidity of atmospheric particles, Atmos. Chem. Phys., 15, 2775-2790, doi:10.5194/acp-15-2775-2015, 2015.

Herrmann, H., Schaefer, T., Tilgner, A., Styler, S. A., Weller, C., Teich, M., and Otto, T.: Tropospheric Aqueous-Phase Chemistry: Kinetics, Mechanisms, and Its Coupling to a Changing Gas Phase, Chem. Rev., 115, 4259-4334, doi:10.1021/cr500447k, 2015.

Ho, K. F., Ho, S. S. H., Lee, S. C., Kawamura, K., Zou, S. C., Cao, J. J., and Xu, H. M.: Summer and winter variations of dicarboxylic acids, fatty acids and benzoic acid in $PM_{2.5}$ in Pearl Delta River Region, China, Atmos. Chem. Phys., 11, 2197-2208, doi:10.5194/acp-11-2197-2011, 2011.

Ho, K. F., Ho, S. S. H., Huang, R. J., Liu, S. X., Cao, J. J., Zhang, T., Chuang, H. C., Chan, C. S., Hu, D., and Tian, L. W.: Characteristics of water-soluble organic nitrogen in fine particulate matter in the continental area of China, Atmos. Environ., 106, 252-261, doi:10.1016/j.atmosenv.2015.02.010, 2015.

Hu, M., Wu, Z., Slanina, J., Lin, P., Liu, S., and Zeng, L.: Acidic gases, ammonia and water-soluble ions in $PM_{2.5}$ at a coastal site in the Pearl River Delta, China, Atmos. Environ., 42, 6310-6320, 2008.

Huang, M., Xu, J., Cai, S., Liu, X., Zhao, W., Hu, C., Gu, X., Fang, L., and Zhang, W.: Characterization of brown carbon constituents of benzene secondary organic aerosol aged with ammonia, J. Atmos. Chem., 75, 205-218, doi:10.1007/s10874-017-9372-x, 2017.

Huang, R. J., Zhang, Y., Bozzetti, C., Ho, K. F., Cao, J. J., Han, Y., Daellenbach, K. R., Slowik, J. G., Platt, S. M., Canonaco, F., Zotter, P., Wolf, R., Pieber, S. M., Bruns, E. A., Crippa, M., Ciarelli, G., Piazzalunga, A., Schwikowski, M., Abbaszade, G., Schnelle-Kreis, J., Zimmermann, R., An, Z., Szidat, S., Baltensperger, U., El Haddad, I., and Prevot, A. S.: High secondary aerosol contribution to particulate pollution during haze events in China, Nature, 514, 218-222, doi:10.1038/nature13774, 2014.

Jeong, C. H., McGuire, M. L., Godri, K. J., Slowik, J. G., Rehbein, P. J. G., and Evans, G. J.: Quantification of aerosol chemical composition using continuous single particle measurements, Atmos. Chem. Phys., 11, 7027-7044, doi:10.5194/acp-11-7027-2011, 2011.

Jia, S. G., Sarkar, S., Zhang, Q., Wang, X. M., Wu, L. L., Chen, W. H., Huang, M. J., Zhou, S. Z., Zhang, J. P., Yuan, L., and Yang, L. M.: Characterization of diurnal variations of PM2.5 acidity using an open thermodynamic system: A case study of Guangzhou, China, Chemosphere, 202, 677-685, doi:10.1016/j.chemosphere.2018.03.127, 2018.

Kampf, C. J., Filippi, A., Zuth, C., Hoffmann, T., and Opatz, T.: Secondary brown carbon formation via the dicarbonyl imine pathway: nitrogen heterocycle formation and synergistic effects, Phys. Chem. Chem. Phys., 18, 18353-18364, doi:10.1039/c6cp03029g, 2016.

Kanakidou, M., Seinfeld, J. H., Pandis, S. N., Barnes, I., Dentener, F. J., Facchini, M. C., Van Dingenen, R., Ervens, B., Nenes, A., Nielsen, C. J., Swietlicki, E., Putaud, J. P., Balkanski, Y., Fuzzi, S., Horth, J., Moortgat, G. K., Winterhalter, R., Myhre, C. E. L., Tsigaridis, K., Vignati, E., Stephanou, E. G., and Wilson, J.: Organic aerosol and global climate modelling: a review, Atmos. Chem. Phys., 5, 1053-1123, 2005.

Kroll, J. H., Ng, N. L., Murphy, S. M., Varutbangkul, V., Flagan, R. C., and Seinfeld, J. H.: Chamber studies of secondary organic aerosol growth by reactive uptake of simple carbonyl compounds, J. Geophys. Res.-Atmos., 110, D23207, doi:10.1029/2005JD006004, 2005.

Laskin, A., Smith, J. S., and Laskin, J.: Molecular Characterization of Nitrogen-Containing Organic Compounds in Biomass Burning Aerosols Using High-Resolution Mass Spectrometry, Environ. Sci. Technol., 43, 3764-3771, doi:10.1021/es803456n, 2009.

Laskin, A., Laskin, J., and Nizkorodov, S. A.: Chemistry of Atmospheric Brown Carbon, Chem. Rev., 115, 4335-4382, doi:10.1021/cr5006167, 2015.

Lee, A. K. Y., Zhao, R., Li, R., Liggio, J., Li, S. M., and Abbatt, J. P. D.: Formation of Light Absorbing Organo-Nitrogen Species from Evaporation of Droplets Containing Glyoxal and Ammonium Sulfate, Environ. Sci. Technol., 47, 12819-12826, doi:10.1021/es402687w, 2013.

Lee, S. H., Murphy, D. M., Thomson, D. S., and Middlebrook, A. M.: Nitrate and oxidized organic ions in single particle mass spectra during the 1999 Atlanta Supersite Project, J. Geophys. Res., 108, 8417, doi:10.1029/2001jd001455, 2003.

Li, J., Fang, Y. T., Yoh, M., Wang, X. M., Wu, Z. Y., Kuang, Y. W., and Wen, D. Z.: Organic nitrogen deposition in precipitation in metropolitan Guangzhou city of southern China, Atmos. Res., 113, 57-67, doi:10.1016/j.atmosres.2012.04.019, 2012.

Li, L., Huang, Z. X., Dong, J. G., Li, M., Gao, W., Nian, H. Q., Fu, Z., Zhang, G. H., Bi, X. H., Cheng, P., and Zhou, Z.: Real time bipolar time-of-flight mass spectrometer for analyzing single aerosol particles, Intl. J. Mass. Spectrom., 303, 118-124, doi:10.1016/j.ijms.2011.01.017, 2011.

Li, X., Rohrer, F., Brauers, T., Hofzumahaus, A., Lu, K., Shao, M., Zhang, Y. H., and Wahner, A.: Modeling of HCHO and CHOCHO at a semi-rural site in southern China during the PRIDE-PRD2006 campaign, Atmos. Chem. Phys., 14, 12291-12305, doi:10.5194/acp-14-12291-2014, 2014.

Li, Z. J., Nizkorodov, S. A., Chen, H., Lu, X. H., Yang, X., and Chen, J. M.: Nitrogen-containing secondary organic aerosol formation by acrolein reaction with ammonia/ammonium, Atmos. Chem. Phys., 19, 1343-1356, doi:10.5194/acp-19-1343-2019, 2019.

Liggio, J., Li, S. M., and Mclaren, R.: Reactive uptake of glyoxal by particulate matter, J. Geophys. Res.-Atmos., 110, D10304, doi:10.1029/2004jd005113, 2005.

Lin, P., Aiona, P. K., Li, Y., Shiraiwa, M., Laskin, J., Nizkorodov, S. A., and Laskin, A.: Molecular Characterization of Brown Carbon in Biomass Burning Aerosol Particles, Environ. Sci. Technol., 50, 11815-11824, doi:10.1021/acs.est.6603024, 2016.

Liu, Y., Liggio, J., Staebler, R., and Li, S. M.: Reactive uptake of ammonia to secondary organic aerosols: kinetics of organonitrogen formation, Atmos. Chem. Phys., 15, 13569-13584, doi:10.5194/acp-15-13569-2015, 2015.

Mace, K. A., Kubilay, N., and Duce, R. A.: Organic nitrogen in rain and aerosol in the eastern Mediterranean atmosphere: An association with atmospheric dust, J. Geophys. Res.-Atmos., 108, 4320, doi:10.1029/2002jd002997, 2003.

563 Miyazaki, Y., Fu, P. Q., Ono, K., Tachibana, E., and Kawamura, K.: Seasonal cycles of
564 water-soluble organic nitrogen aerosols in a deciduous broadleaf forest in northern Japan, J.
565 Geophys. Res.-Atmos., 119, 1440-1454, doi:10.1002/2013JD020713, 2014.
566 Mohr, C., Lopez-Hilfiker, F. D., Zotter, P., Prévôt, A. S. H., Xu, L., Ng, N. L., Herndon,
567 S. C., Williams, L. R., Franklin, J. P., Zahniser, M. S., Worsnop, D. R., Knighton, W. B., Aiken,
568 A. C., Gorkowski, K. J., Dubey, M. K., Allan, J. D., and Thornton, J. A.: Contribution of
569 Nitrated Phenols to Wood Burning Brown Carbon Light Absorption in Detling, United
570 Kingdom during Winter Time, Environ. Sci. Technol., 47, 6316-6324, doi:10.1021/es400683v,
571 2013.
572 Moise, T., Flores, J. M., and Rudich, Y.: Optical Properties of Secondary Organic Aerosols
573 and Their Changes by Chemical Processes, Chem. Rev., 115, 4400-4439,
574 doi:10.1021/cr5005259, 2015.
575 Murphy, J. G., Gregoire, P. K., Tevlin, A. G., Wentworth, G. R., Ellis, R. A., Markovic,
576 M. Z., and VandenBoer, T. C.: Observational constraints on particle acidity using
577 measurements and modelling of particles and gases, Faraday Discuss., 200, 379-395,
578 doi:10.1039/c7fd00086c, 2017.
579 Neff, J. C., Holland, E. A., Dentener, F. J., McDowell, W. H., and Russell, K. M.: The
580 origin, composition and rates of organic nitrogen deposition: A missing piece of the nitrogen
581 cycle?, Biogeochemistry, 57, 99-136, 2002.
582 Nguyen, T. B., Lee, P. B., Updyke, K. M., Bones, D. L., Laskin, J., Laskin, A., and
583 Nizkorodov, S. A.: Formation of nitrogen- and sulfur-containing light-absorbing compounds
584 accelerated by evaporation of water from secondary organic aerosols, J. Geophys. Res.-Atmos.,
585 117, D01207, doi:10.1029/2011jd016944, 2012.
586 Norris, G., Vedantham, R., Wade, K., Zahn, P., Brown, S., Paatero, P., Eberly, S., and
587 Foley, C. (2009), Guidance document for PMF applications with the Multilinear Engine, edited,
588 Prepared for the U.S. Environmental Protection Agency, Research Triangle Park, NC.

589 Noziere, B., Dziedzic, P., and Cordova, A.: Products and Kinetics of the Liquid-Phase
590 Reaction of Glyoxal Catalyzed by Ammonium Ions (NH_4^+), J. Phys. Chem. A, 113, 231-237,
591 doi:10.1021/jp8078293, 2009.
592 Ortiz-Montalvo, D. L., Hakkinen, S. A. K., Schwier, A. N., Lim, Y. B., McNeill, V. F.,
593 and Turpin, B. J.: Ammonium Addition (and Aerosol pH) Has a Dramatic Impact on the
594 Volatility and Yield of Glyoxal Secondary Organic Aerosol, Environ. Sci. Technol., 48, 255-
595 262, doi:10.1021/es4035667, 2014.
596 Pagels, J., Dutcher, D. D., Stolzenburg, M. R., McMurry, P. H., Galli, M. E., and Gross,
597 D. S.: Fine-particle emissions from solid biofuel combustion studied with single-particle mass
598 spectrometry: Identification of markers for organics, soot, and ash components, J. Geophys.
599 Res.-Atmos., 118, 859-870, doi:10.1029/2012jd018389, 2013.
600 Pan, Y. P., Tian, S. L., Zhao, Y. H., Zhang, L., Zhu, X. Y., Gao, J., Huang, W., Zhou, Y.
601 B., Song, Y., Zhang, Q., and Wang, Y. S.: Identifying Ammonia Hotspots in China Using a
602 National Observation Network, Environ. Sci. Technol., 52, 3926-3934,
603 doi:10.1021/acs.est.7b05235, 2018.
604 Paulot, F., Wunch, D., Crounse, J. D., Toon, G. C., Millet, D. B., DeCarlo, P. F.,
605 Vigouroux, C., Deutscher, N. M., González Abad, G., Notholt, J., Warneke, T., Hannigan, J.
606 W., Warneke, C., de Gouw, J. A., Dunlea, E. J., De Mazière, M., Griffith, D. W. T., Bernath,
607 P., Jimenez, J. L., and Wennberg, P. O.: Importance of secondary sources in the atmospheric
608 budgets of formic and acetic acids, Atmos. Chem. Phys., 11, 1989-2013, doi:10.5194/acp-11-
609 1989-2011, 2011.
610 Qin, X. Y., Bhave, P. V., and Prather, K. A.: Comparison of two methods for obtaining
611 quantitative mass concentrations from aerosol time-of-flight mass spectrometry measurements,
612 Anal. Chem., 78, 6169-6178, doi:10.1021/ac060395q, 2006.
613 Rastogi, N., Zhang, X., Edgerton, E. S., Ingall, E., and Weber, R. J.: Filterable water-
614 soluble organic nitrogen in fine particles over the southeastern USA during summer, Atmos.
615 Environ., 45, 6040-6047, doi:10.1016/j.atmosenv.2011.07.045, 2011.

Sareen, N., Schwier, A. N., Shapiro, E. L., Mitroo, D., and McNeill, V. F.: Secondary organic material formed by methylglyoxal in aqueous aerosol mimics, Atmos. Chem. Phys., 10, 997-1016, doi:10.5194/acp-10-997-2010, 2010.

Sedehi, N., Takano, H., Blasic, V. A., Sullivan, K. A., and De Haan, D. O.: Temperature- and pH-dependent aqueous-phase kinetics of the reactions of glyoxal and methylglyoxal with atmospheric amines and ammonium sulfate, Atmos. Environ., 77, 656-663, doi:10.1016/j.atmosenv.2013.05.070, 2013.

Seinfeld, J. H., and Pandis, S. N.: Atmospheric Chemistry and Physics: From Air Pollution to Climate Change, edited by: John Wiley&Sons, I., John Wiley&Sons, Inc., New Jersey, 2006.

Shapiro, E. L., Szprengiel, J., Sareen, N., Jen, C. N., Giordano, M. R., and McNeill, V. F.: Light-absorbing secondary organic material formed by glyoxal in aqueous aerosol mimics, Atmos. Chem. Phys., 9, 2289-2300, 2009.

Shi, J., Gao, H., Qi, J., Zhang, J., and Yao, X.: Sources, compositions, and distributions of water-soluble organic nitrogen in aerosols over the China Sea, J. Geophys. Res.-Atmos., 115, D17303, doi:10.1029/2009jd013238, 2010.

Shrivastava, M., Cappa, C. D., Fan, J. W., Goldstein, A. H., Guenther, A. B., Jimenez, J. L., Kuang, C., Laskin, A., Martin, S. T., Ng, N. L., Petaja, T., Pierce, J. R., Rasch, P. J., Roldin, P., Seinfeld, J. H., Shilling, J., Smith, J. N., Thornton, J. A., Volkamer, R., Wang, J., Worsnop, D. R., Zaveri, R. A., Zelenyuk, A., and Zhang, Q.: Recent advances in understanding secondary organic aerosol: Implications for global climate forcing, Rev. Geophys., 55, 509-559, doi:10.1002/2016RG000540, 2017.

Silva, P. J., and Prather, K. A.: Interpretation of mass spectra from organic compounds in aerosol time-of-flight mass spectrometry, Anal. Chem., 72, 3553-3562, 2000.

Sullivan, R. C., and Prather, K. A.: Investigations of the diurnal cycle and mixing state of oxalic acid in individual particles in Asian aerosol outflow, Environ. Sci. Technol., 41, 8062-8069, 2007.

Sun, J. Z., Zhi, G. R., Hitzenberger, R., Chen, Y. J., Tian, C. G., Zhang, Y. Y., Feng, Y. L., Cheng, M. M., Zhang, Y. Z., Cai, J., Chen, F., Qiu, Y., Jiang, Z., Li, J., Zhang, G., and Mo,

Y.: Emission factors and light absorption properties of brown carbon from household coal combustion in China, Atmos. Chem. Phys., 17, 4769-4780, doi:10.5194/acp-17-4769-2017, 2017.

Sun, Y. L., Zhang, Q., Schwab, J. J., Demerjian, K. L., Chen, W. N., Bae, M. S., Hung, H. M., Hogrefe, O., Frank, B., Rattigan, O. V., and Lin, Y. C.: Characterization of the sources and processes of organic and inorganic aerosols in New York city with a high-resolution time-of-flight aerosol mass apectrometer, Atmos. Chem. Phys., 11, 1581-1602, doi:10.5194/acp-11-1581-2011, 2011.

Teich, M., van Pinxteren, D., Kecorius, S., Wang, Z. B., and Herrmann, H.: First Quantification of Imidazoles in Ambient Aerosol Particles: Potential Photosensitizers, Brown Carbon Constituents, and Hazardous Components, Environ. Sci. Technol., 50, 1166-1173, doi:10.1021/acs.est.5b05474, 2016.

Updyke, K. M., Nguyen, T. B., and Nizkorodov, S. A.: Formation of brown carbon via reactions of ammonia with secondary organic aerosols from biogenic and anthropogenic precursors, Atmos. Environ., 63, 22-31, doi:10.1016/j.atmosenv.2012.09.012, 2012.

Wang, X. F., Gao, S., Yang, X., Chen, H., Chen, J. M., Zhuang, G. S., Surratt, J. D., Chan, M. N., and Seinfeld, J. H.: Evidence for High Molecular Weight Nitrogen-Containing Organic Salts in Urban Aerosols, Environ. Sci. Technol., 44, 4441-4446, 2010.

Wang, X. F., Wang, H. L., Jing, H., Wang, W. N., Cui, W. D., Williams, B. J., and Biswas, P.: Formation of Nitrogen-Containing Organic Aerosol during Combustion of High-Sulfur-Content Coal, Energ. Fuel., 31, 14161-14168, doi:10.1021/acs.energyfuels.7b02273, 2017.

Woo, J. L., Kim, D. D., Schwier, A. N., Li, R. Z., and McNeill, V. F.: Aqueous aerosol SOA formation: impact on aerosol physical properties, Faraday Discuss., 165, 357-367, doi:10.1039/c3fd00032j, 2013.

Xu, L., Guo, H. Y., Boyd, C. M., Klein, M., Bougiatioti, A., Cerully, K. M., Hite, J. R., Isaacman-VanWertz, G., Kreisberg, N. M., Knote, C., Olson, K., Koss, A., Goldstein, A. H., Hering, S. V., de Gouw, J., Baumann, K., Lee, S. H., Nenes, A., Weber, R. J., and Ng, N. L.: Effects of anthropogenic emissions on aerosol formation from isoprene and monoterpenes in

672 the southeastern United States, Proc. Natl. Acad. Sci. USA, 112, E4509-E4509,
673 doi:10.1073/pnas.1512279112, 2015.
674 Xu, W. Q., Sun, Y. L., Wang, Q. Q., Du, W., Zhao, J., Ge, X. L., Han, T. T., Zhang, Y. J.,
675 Zhou, W., Li, J., Fu, P. Q., Wang, Z. F., and Worsnop, D. R.: Seasonal Characterization of
676 Organic Nitrogen in Atmospheric Aerosols Using High Resolution Aerosol Mass Spectrometry
677 in Beijing, China, ACS Earth Space Chem., 1, 673-682,
678 doi:10.1021/acsearthspacechem.7b00106, 2017.
679 Yan, J., Wang, X., Gong, P., Wang, C., and Cong, Z.: Review of brown carbon aerosols:
680 Recent progress and perspectives, Sci. Total. Environ., 634, 1475-1485,
681 doi:10.1016/j.scitotenv.2018.04.083, 2018.
682 Yu, X., Yu, Q. Q., Zhu, M., Tang, M. J., Li, S., Yang, W. Q., Zhang, Y. L., Deng, W., Li,
683 G. H., Yu, Y. G., Huang, Z. H., Song, W., Ding, X., Hu, Q. H., Li, J., Bi, X. H., and Wang, X.
684 M.: Water Soluble Organic Nitrogen (WSON) in Ambient Fine Particles Over a Megacity in
685 South China: Spatiotemporal Variations and Source Apportionment, J. Geophys. Res.-Atmos.,
686 122, 13045-13060, doi:10.1002/2017JD027327, 2017.
687 Yuan, B., Liggio, J., Wentzell, J., Li, S. M., Stark, H., Roberts, J. M., Gilman, J., Lerner,
688 B., Warneke, C., Li, R., Leithead, A., Osthoff, H. D., Wild, R., Brown, S. S., and de Gouw, J.
689 A.: Secondary formation of nitrated phenols: insights from observations during the Uintah
690 BasinWinter Ozone Study (UBWOS) 2014, Atmos. Chem. Phys., 16, 2139-2153,
691 doi:10.5194/acp-16-2139-2016, 2016.
692 Yuan, Q., Lai, S., Song, J., Ding, X., Zheng, L., Wang, X., Zhao, Y., Zheng, J., Yue, D.,
693 Zhong, L., Niu, X., and Zhang, Y.: Seasonal cycles of secondary organic aerosol tracers in rural
694 Guangzhou, Southern China: The importance of atmospheric oxidants, Environ. Pollut., 240,
695 884-893, doi:10.1016/j.envpol.2018.05.009, 2018.
696 Zauscher, M. D., Wang, Y., Moore, M. J. K., Gaston, C. J., and Prather, K. A.: Air Quality
697 Impact and Physicochemical Aging of Biomass Burning Aerosols during the 2007 San Diego
698 Wildfires, Environ. Sci. Technol., 47, 7633-7643, doi:10.1021/es4004137, 2013.

Zawadowicz, M. A., Froyd, K. D., Murphy, D. M., and Cziczo, D. J.: Improved identification of primary biological aerosol particles using single-particle mass spectrometry, Atmos. Chem. Phys., 17, 7193-7212, doi:10.5194/acp-17-7193-2017, 2017.

Zhang, G., Lin, Q., Peng, L., Yang, Y., Jiang, F., Liu, F., Song, W., Chen, D., Cai, Z., Bi, X., Miller, M., Tang, M., Huang, W., Wang, X., Peng, P., and Sheng, G.: Oxalate Formation Enhanced by Fe-Containing Particles and Environmental Implications, Environ. Sci. Technol., 53, 1269-1277, doi:10.1021/acs.est.8b05280, 2019.

Zhang, G. H., Bi, X. H., He, J. J., Chen, D. H., Chan, L. Y., Xie, G. W., Wang, X. M., Sheng, G. Y., Fu, J. M., and Zhou, Z.: Variation of secondary coatings associated with elemental carbon by single particle analysis, Atmos. Environ., 92, 162-170, doi:10.1016/j.atmosenv.2014.04.018, 2014.

Zhang, G. H., Lin, Q. H., Peng, L., Yang, Y. X., Fu, Y. Z., Bi, X. H., Li, M., Chen, D. H., Chen, J. X., Cai, Z., Wang, X. M., Peng, P. A., Sheng, G. Y., and Zhou, Z.: Insight into the in-cloud formation of oxalate based on in situ measurement by single particle mass spectrometry, Atmos. Chem. Phys., 17, 13891-13901, doi:10.5194/acp-17-13891-2017, 2017.

Zhang, H. F., Yee, L. D., Lee, B. H., Curtis, M. P., Worton, D. R., Isaacman-VanWertz, G., Offenberg, J. H., Lewandowski, M., Kleindienst, T. E., Beaver, M. R., Holder, A. L., Lonneman, W. A., Docherty, K. S., Jaoui, M., Pye, H. O. T., Hu, W. W., Day, D. A., Campuzano-Jost, P., Jimenez, J. L., Guo, H. Y., Weber, R. J., de Gouw, J., Koss, A. R., Edgerton, E. S., Brune, W., Mohr, C., Lopez-Hilfiker, F. D., Lutz, A., Kreisberg, N. M., Spielman, S. R., Hering, S. V., Wilson, K. R., Thornton, J. A., and Goldstein, A. H.: Monoterpenes are the largest source of summertime organic aerosol in the southeastern United States, Proc. Natl. Acad. Sci. USA, 115, 2038-2043, doi:10.1073/pnas.1717513115, 2018.

Zhang, Q., Duan, F., He, K., Ma, Y., Li, H., Kimoto, T., and Zheng, A.: Organic nitrogen in PM2.5 in Beijing, Frontiers of Environmental Science & Engineering, 9, 1004-1014, doi:10.1007/s11783-015-0799-5, 2015.

Zhang, Y. S., Shao, M., Lin, Y., Luan, S. J., Mao, N., Chen, W. T., and Wang, M.: Emission inventory of carbonaceous pollutants from biomass burning in the Pearl River Delta Region, China, Atmos. Environ., 76, 189-199, doi:10.1016/j.atmosenv.2012.05.055, 2013.

Zhao, R., Lee, A. K. Y., and Abbatt, J. P. D.: Investigation of Aqueous-Phase Photooxidation of Glyoxal and Methylglyoxal by Aerosol Chemical Ionization Mass Spectrometry: Observation of Hydroxyhydroperoxide Formation, J. Phys. Chem. A, 116, 6253-6263, doi:10.1021/jp211528d, 2012.

Zhao, R., Lee, A. K. Y., Huang, L., Li, X., Yang, F., and Abbatt, J. P. D.: Photochemical processing of aqueous atmospheric brown carbon, Atmos. Chem. Phys., 15, 6087-6100, doi:10.5194/acp-15-6087-2015, 2015.

Zheng, J. Y., Yin, S. S., Kang, D. W., Che, W. W., and Zhong, L. J.: Development and uncertainty analysis of a high-resolution NH_3 emissions inventory and its implications with precipitation over the Pearl River Delta region, China, Atmos. Chem. Phys., 12, 7041-7058, doi:10.5194/acp-12-7041-2012, 2012.

Zhou, S. Z., Wang, T., Wang, Z., Li, W. J., Xu, Z., Wang, X. F., Yuan, C., Poon, C. N., Louie, P. K. K., Luk, C. W. Y., and Wang, W. X.: Photochemical evolution of organic aerosols observed in urban plumes from Hong Kong and the Pearl River Delta of China, Atmos. Environ., 88, 219-229, doi:10.1016/j.atmosenv.2014.01.032, 2014.

Zhou, Y., Huang, X. H. H., Griffith, S. M., Li, M., Li, L., Zhou, Z., Wu, C., Meng, J. W., Chan, C. K., Louie, P. K. K., and Yu, J. Z.: A field measurement based scaling approach for quantification of major ions, organic carbon, and elemental carbon using a single particle aerosol mass spectrometer, Atmos. Environ., 143, 300-312, doi:10.1016/j.atmosenv.2016.08.054, 2016.

Zhu, S. P., Horne, J. R., Montoya-Aguilera, J., Hinks, M. L., Nizkorodov, S. A., and Dabdub, D.: Modeling reactive ammonia uptake by secondary organic aerosol in CMAQ: application to the continental US, Atmos. Chem. Phys., 18, 3641-3657, doi:10.5194/acp-18-3641-2018, 2018.

752 Ziemann, P. J., and Atkinson, R.: Kinetics, products, and mechanisms of secondary
753 organic aerosol formation, Chem. Soc. Rev., 41, 6582-6605, doi:10.1039/c2cs35122f, 2012.
754

Figure captions

Figure 1. Representative mass spectrum for NOC-containing particles. The ion peaks corresponding to NOCs and oxidized organics are highlighted with red bars.

Figure 2. The variation in hourly mean Nfs of the oxidized organics and ammonium that internally mixed with NOCs. Box and whisker plot shows lower, median, and upper lines, denoting the 25^{th}, 50^{th}, and 75^{th} percentiles, respectively; the lower and upper edges denote the 10^{th} and 90^{th} percentiles, respectively.

Figure 3. Correlation analysis of (a, c) the RPAs and (b, d) the number of detected NOCs, with the oxidized organics and ammonium in different seasons. Significant ($p < 0.01$) correlations were obtained for both the total observed data and the seasonally separated data. RPA is defined as the fractional peak area of each *m/z* relative to the sum of peak areas in the mass spectrum and is applied to represent the relative amount of a species on a particle (Jeong et al., 2011; Healy et al., 2013).

Figure 4. Comparison between the measured and predicted RPAs for NOCs.

Figure 5. (left) PMF-resolved 3-factor source profiles (percentage of total species) and (right) their diurnal variations (arbitrary unit).

Figure 6. The dependence of NOCs and the ratio of NOCs to the oxidized organics on RH and NOx.

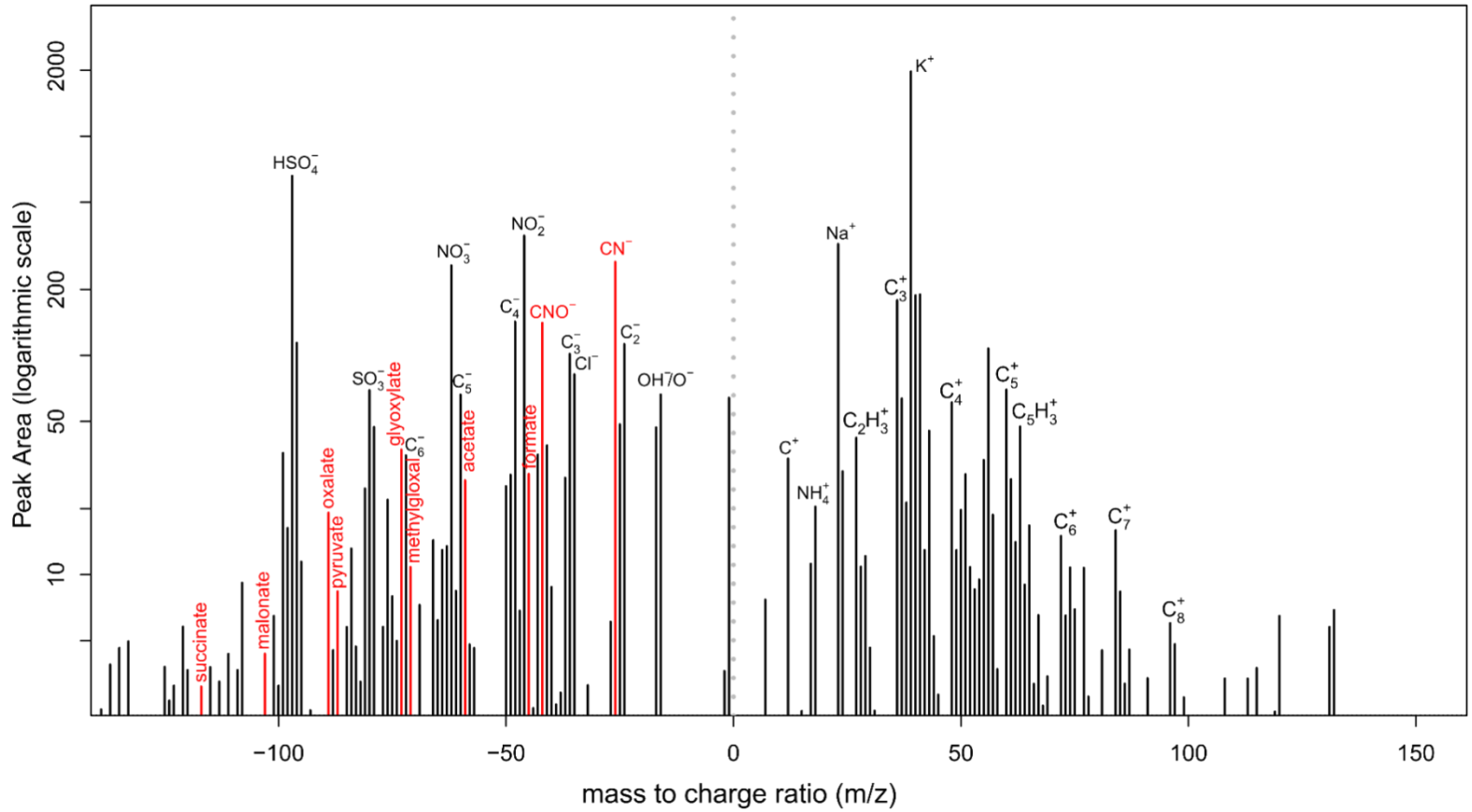
Peak Area (logarithmic scale)
10
50
200
2000
mass to charge ratio (m/z)
−100
−50
0
50
100
150
HSO4−
SO3−
NO3−
NO2−
C4−
CNO−
C3−
Cl−
CN−
C2−
OH−/O−
C5−
glyoxylate
C6−
methylglioxal
oxalate
pyruvate
malonate
succinate
acetate
formate
C+
NH4+
Na+
C2H3+
C3+
K+
C4+
C5+
C5H3+
C6+
C7+
C8+

773

774 Fig. 1.

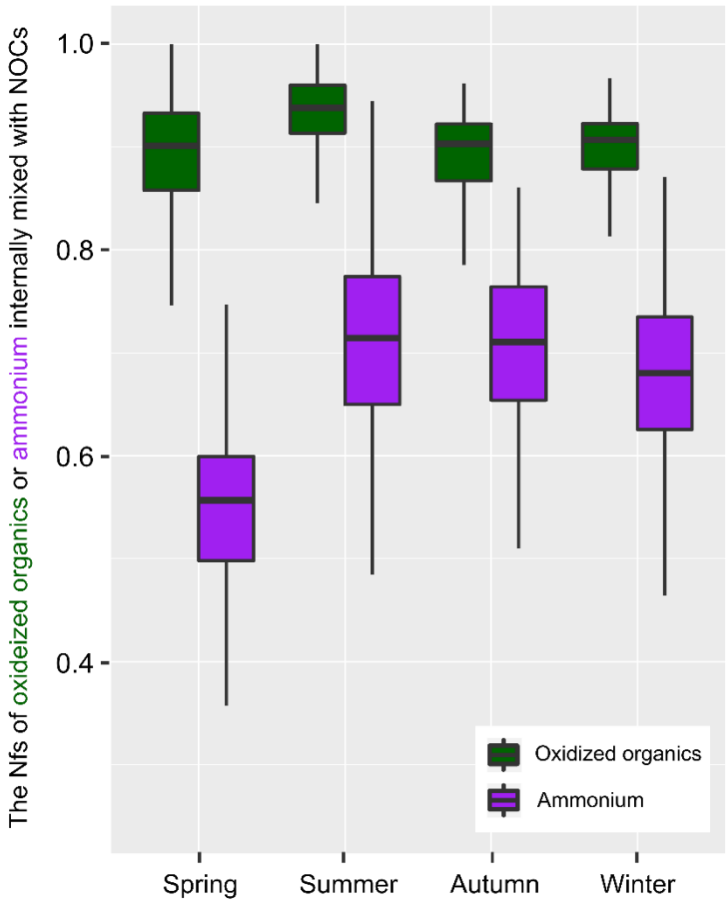

775

776 Fig. 2.

777

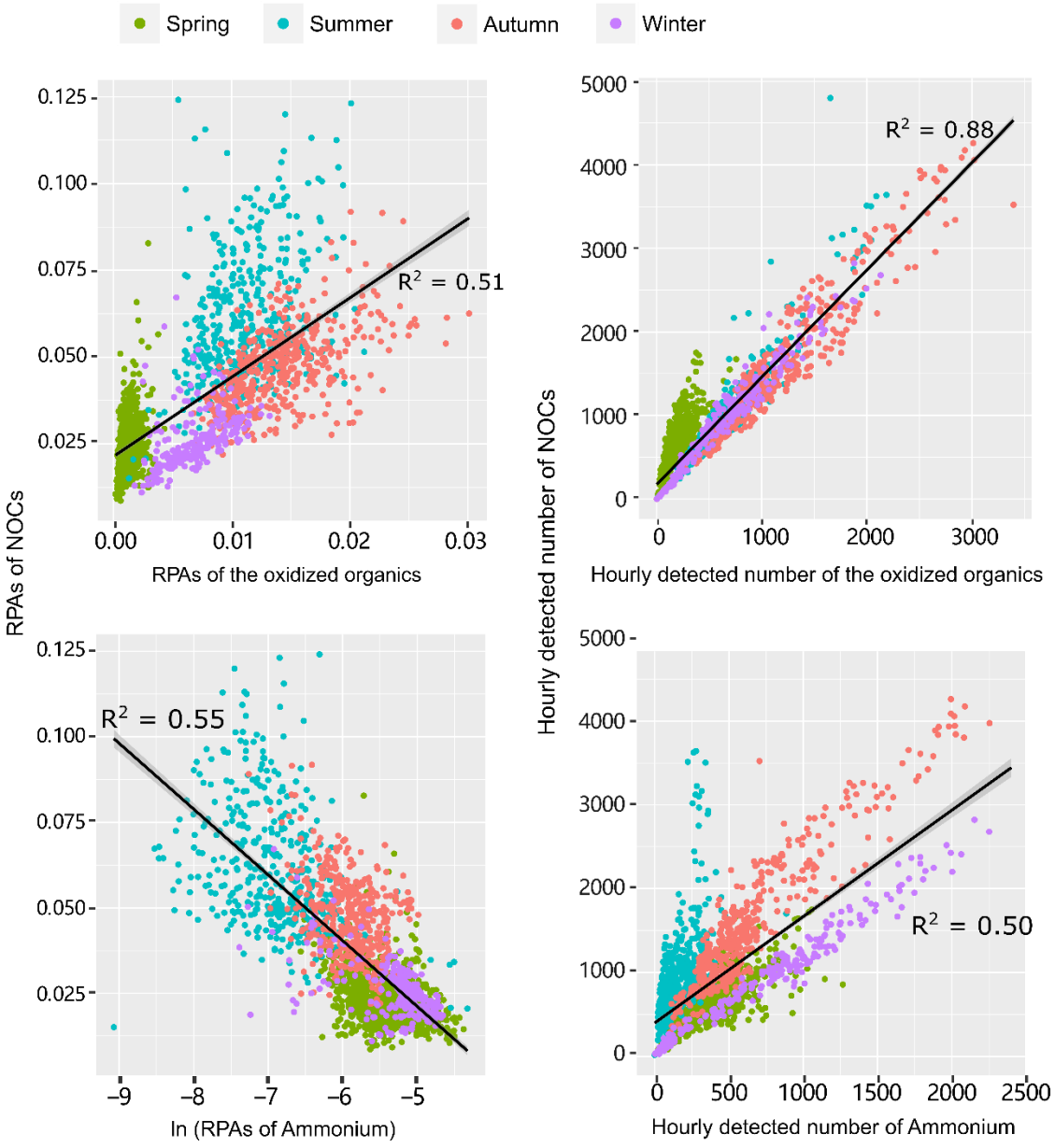
Spring
Summer
Autumn
Winter
RPAs of NOCs
RPAs of the oxidized organics
R² = 0.51
Hourly detected number of NOCs
Hourly detected number of the oxidized organics
R² = 0.88
ln (RPAs of Ammonium)
R² = 0.55
Hourly detected number of Ammonium
R² = 0.50

778

779 Fig. 3.

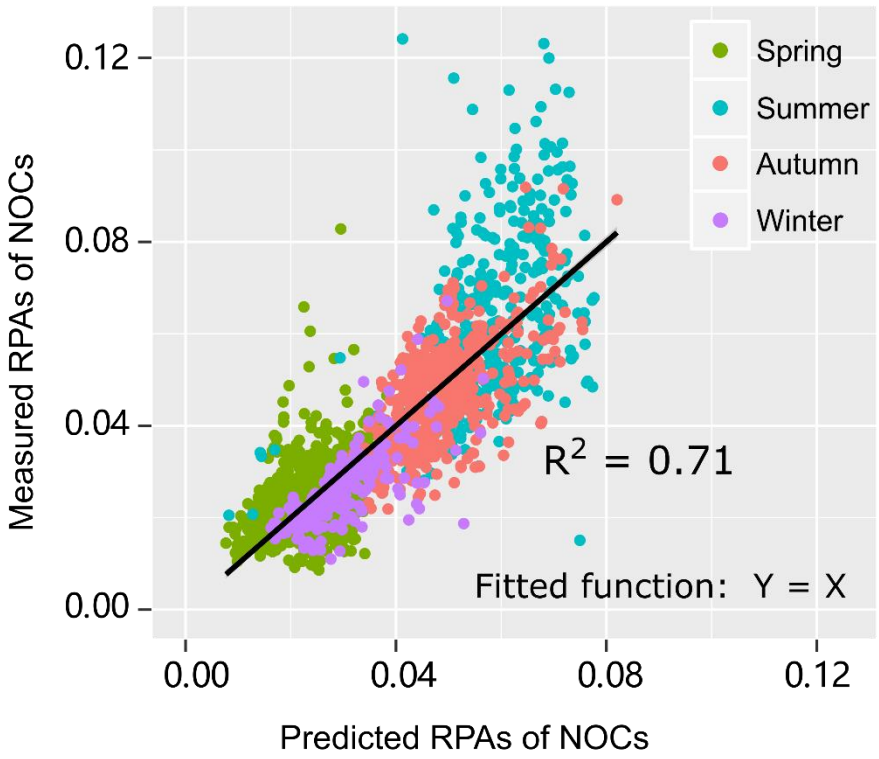
Spring
Summer
Autumn
Winter
0.12
0.08
0.04
0.00
Measured RPAs of NOCs
R2 = 0.71
Fitted function: Y = X
0.00
0.04
0.08
0.12
Predicted RPAs of NOCs

780

781 **Fig. 4.**

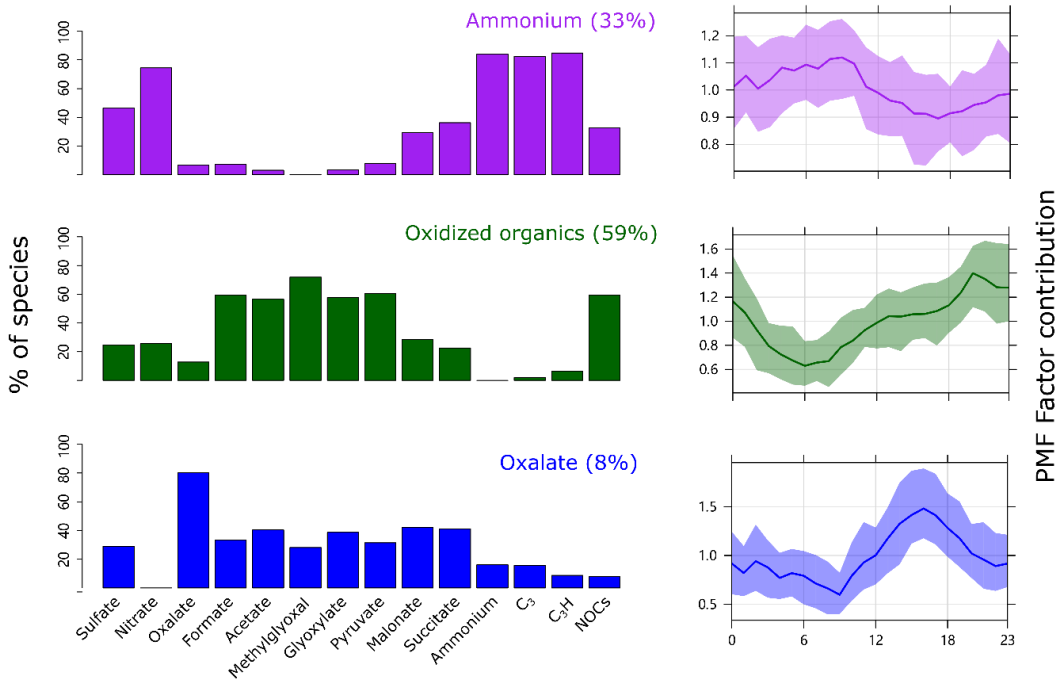
Ammonium (33%)
Oxidized organics (59%)
Oxalate (8%)
% of species
PMF Factor contribution
Sulfate
Nitrate
Oxalate
Formate
Acetate
Methylglyoxal
Glyoxylate
Pyruvate
Malonate
Succitate
Ammonium
C5
C5H
NOCs

Fig. 5.

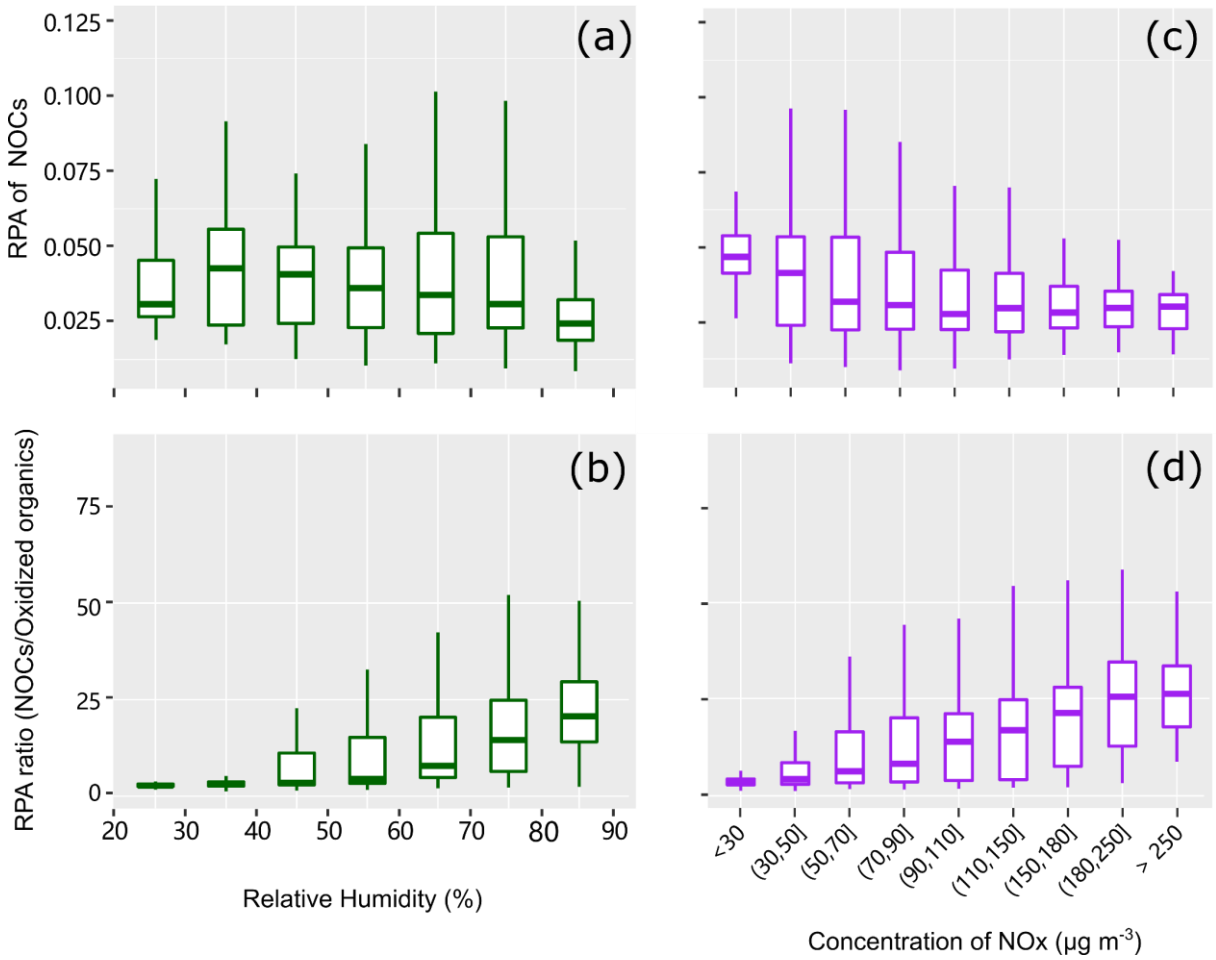
(a)
(b)
(c)
(d)
RPA of NOCs
RPA ratio (NOCs/Oxidized organics)
0.125
0.100
0.075
0.050
0.025
75
50
25
0
20
30
40
50
60
70
80
90
Relative Humidity (%)
<30
(30,50]
(50,70]
(70,90]
(90,110]
(110,150]
(150,180]
(180,250]
> 250
Concentration of NOx (µg m-3)

786

787 **Fig. 6.**